6-1-2007

The Physical Origin Of Negative Superhumps In Cataclysmic Variables

Matt A. Wood

Christopher J. Burke

The Astrophysical Journal, 661:1042–1047, 2007 June 1

THE PHYSICAL ORIGIN OF NEGATIVE SUPERHUMPS IN CATACLYSMIC VARIABLES

Matt A. Wood
Department of Physics and Space Sciences, and SARA Observatory, Florida Institute of Technology, Melbourne, FL 32901; wood@fit.edu

and

Christopher J. Burke
Space Telescope Science Institute, Baltimore, MD 21208; cjburke@stsci.edu
Received 2006 November 8; accepted 2007 February 20

ABSTRACT

It has been suspected for over 20 years that the observed negative superhumps in cataclysmic variables are due to the retrograde precession of a tilted disk. We present new smooth particle hydrodynamics simulation results that demonstrate that the source of the modulation of the luminosity of the light in a negatively superhumping cataclysmic variable is the transit of the bright spot across the face of an accretion disk that is tilted out of the orbital plane. In an untilted disk the bright spot is always located on the outer edge of the disk, and the intrinsic brightness of the accretion spot is constant for a disk at equilibrium. However, if the accretion disk is tilted out of the orbital plane and only slowly precessing in the inertial frame, then the bright spot will have this luminosity just twice per orbit as the accretion stream impacts the disk edge at the line of nodes. At other times, however, the accretion spot will transit across one face or the other of the tilted disk as the secondary star moves in orbit. Because the impact point is then deeper in the gravitational potential well of the primary white dwarf, the bright spot luminosity is correspondingly higher. Because only one face of the disk is visible in these optically thick disk systems, only one brightening per orbit is observed, and the slow retrograde precession of the tilted disk results in a period slightly shorter than the orbital period. We present simulation light curves and an animation to demonstrate these results.

Subject headings: accretion, accretion disks — binaries: close — hydrodynamics — methods: numerical — novae, cataclysmic variables

Online material: mpeg animation

1. INTRODUCTION

Cataclysmic variable (CV) systems are short-period mass-transfer binary systems consisting of a white dwarf primary (M_1) and (typically) a lower main-sequence secondary (M_2). The orbital separation is small enough that the secondary fills its Roche lobe, and it loses mass through the inner Lagrange point (L1). Typical mass-transfer rates are in the range $\dot{M} \sim 10^{-11}$ to $\sim 10^{-7}\ M_\odot\ \mathrm{yr}^{-1}$. Conservation of angular momentum and the small size of the primary preclude the mass stream impacting the primary directly. Instead, an accretion disk forms in which the orbital speed at a given radius within the disk is the expected Keplerian value. The fluid viscosity within the accretion disk acts to transport angular momentum outward in radius, allowing mass to migrate inward through the disk and onto the white dwarf. The most luminous components in a typical high-$\dot{M}$ CV are (1) the bright spot, where the accretion stream impacts the disk, (2) the disk itself, and (3) the boundary layer where the disk plasma settles onto the surface of the accreting white dwarf. The ultimate source of luminosity is the release of gravitational potential energy. Cataclysmic variables are discussed in great detail in Warner (1995) and Hellier (2001).

Several kinds of cataclysmic variables exhibit superhumps, which are photometric modulations near, but not at, the orbital period. Superhumps were first discovered among the SU UMa–type dwarf novae. In these systems superhumps develop during superoutbursts, which are both brighter and longer lived than typical outbursts. The superhump oscillations are observed to have periods P_+ (denoting positive superhumps) a few percent longer than the orbital period, where the so-called superhump period excess $\varepsilon_+ = (P_+ - P_{\mathrm{orb}})/P_{\mathrm{orb}}$ is found to be a function of system mass ratio $q \equiv M_2/M_1$ (Baker-Branstetter & Wood 1999; Patterson 2001; Patterson et al. 2002, 2005; Montgomery 2004, and references therein). The nature of the superhump oscillations were solved by Whitehurst and collaborators (Whitehurst 1988, 1994; Hirose & Osaki 1990; Whitehurst & King 1991). They showed that the SU UMa systems were dwarf nova systems that had mass ratios $q \lesssim 0.25$, such that the 3 : 1 corotation resonance (and associated inner Lindblad resonance) is contained within the Roche lobe of the white dwarf primary (Lubow 1991a, 1991b). Later simulations (Baker-Branstetter & Wood 1999; Montgomery 2001) showed that superhumps could be excited in systems up to a mass ratio $q = 0.34$, a result tentatively confirmed by observations of BB Doradus (Patterson et al. 2005). Normal dwarf nova outbursts in which disk viscosity increases dramatically on a short timescale via the disk instability mechanism increase the overall disk radius, and after a few such outbursts, the outer disk radius can reach the inner Lindblad resonance. The rotating tidal field of the secondary then drives a disk oscillation at a frequency slightly longer than the orbital period (the superhump period P_+) and the periodically changing disk geometry leads to viscous dissipation observed as the superhump signal (Warner 1995; Simpson & Wood 1998). In Wood et al. (2006), we make available for general use a user-friendly demonstration version of our research code so nonspecialists can simulate and visualize accretion disk dynamics including positive superhumps.

The story of superhumps became more complicated with the discovery of the 5.2 hr photometric period in the $P_{\mathrm{orb}} = 5.5$ hr cataclysmic variable TV Col (Bonnet-Bidaud et al. 1985). These authors suggested that the $\sim$4 day beat period between the 5.2 and 5.5 hr periods was consistent with the *retrograde* precession period of an accretion disk tilted out of the orbital plane. Barrett

et al. (1988) followed up with a study of TV Col in which they agreed that the system contained a freely precessing accretion disk, and that the source of the disk tilt might be a relatively strong magnetic field on the secondary star diverting the flow through L1 out of the orbital plane. Barrett et al. also presciently suggested that the source of the negative superhump light curve might be the accretion stream impacting and sweeping across the face of the tilted disk, a model which seems to have been largely overlooked in subsequent years, but which we are able to confirm with our simulation results below.

Since the preliminary results on TV Col, a handful of additional systems have been found to display so-called negative superhumps (period P_-), including V603 Aql, V503 Cyg, V1159 Ori, TT Ari, V751 Cyg, V442 Oph, and AM CVn. Patterson et al. (1993) discussed the systems as a class and showed the superhump period "deficit" $\varepsilon_- \sim (P_- - P_{\rm orb})/P_{\rm orb}$ as a function of orbital period has a magnitude roughly half that of the superhump period excess at a given orbital period (also see Patterson 1999; Wood et al. 2000; Montgomery 2004). The *full* nature of negative superhumps and how they can coexist with positive superhumps has remained elusive since their discovery.

In § 2, we discuss the calculations we have completed for this work, and in § 3, we present our results. We discuss our findings in the context of observed systems that display negative superhumps in § 4.

2. THE SIMULATIONS

2.1. *Numerics*

We use the smoothed particle hydrodynamics (SPH) code developed by Simpson (1995) and Simpson & Wood (1998, hereafter SW98), which we now call FITDisk (see also Wood et al. 2006). SPH is a powerful approach to highly dynamic astrophysical fluid simulations (Lucy 1977; Benz 1991; Monaghan 1992), because the computational elements ("particles") follow the fluid flow. Kernel interpolation over a limited smoothing length h is used to calculate field quantities and gradients. The kernel could be any general function that peaks at the particle location and falls off to zero at large distances (a Gaussian, for example), but it is common practice to use a kernel which is similar in shape to a Gaussian, but which has compact support, going identically to zero beyond a distance $2\,h$ (Monaghan & Lattanzio 1985). Our code FITDisk is typical in that it models only the hydrodynamics of an ideal gamma-law ideal gas equation of state $P = (\gamma - 1)\rho u$, where we typically assume $\gamma = 1.01$. Within this model the sound speed is $c_s = [\gamma(\gamma - 1)u]^{1/2}$. We do not include radiative transfer or magnetic fields in the equations we solve, and we keep h constant for all particles for computational efficiency. Particles have individual time steps that are as long as $\delta t_0 = 0.005 P_{\rm orb}$, or as short as $\delta t_0/128$, as indicated by the local conditions for the particle.

The momentum and energy equations in their general form including gravitational body forces are (SW98)

$$\frac{d^2\boldsymbol{r}}{dt^2} = -\frac{\nabla P}{\rho} + \boldsymbol{f}_{\rm visc} - \frac{GM_1}{r_1^3}\boldsymbol{r}_1 - \frac{GM_2}{r_2^3}\boldsymbol{r}_2, \tag{1}$$

$$\frac{du}{dt} = -\frac{P}{\rho}\nabla \cdot \boldsymbol{v} + \epsilon_{\rm visc}, \tag{2}$$

where P is the pressure, ρ is the density, u is the specific internal energy, $\boldsymbol{f}_{\rm visc}$ is the viscous force, $\epsilon_{\rm visc}$ is the energy generation from viscous dissipation, and $\boldsymbol{r}_{1,2} \equiv \boldsymbol{r} - \boldsymbol{r}_{M1,M2}$ are the displacements from the stellar masses M_1 and M_2, respectively.

Our SPH form of the momentum equation for a particle i is given by

$$\frac{d^2\boldsymbol{r}_i}{dt^2} = -\sum_j m_j\left(\frac{P_i}{\rho_i^2} + \frac{P_j}{\rho_j^2}\right)(1 + \Pi_{ij})\nabla_i W_{ij} - \frac{GM_1}{r_{i1}^3}\boldsymbol{r}_{i1} - \frac{GM_2}{r_{i2}^3}\boldsymbol{r}_{i2}, \tag{3}$$

where we adopt the artificial viscosity approximation of Lattanzio et al. (1986) evaluated between particles i and j,

$$\Pi_{ij} = \begin{cases} -\alpha\mu_{ij} + \beta\mu_{ij}^2, & \boldsymbol{v}_{ij}\cdot\boldsymbol{r}_{ij} \le 0, \\ 0, & \text{otherwise}, \end{cases} \tag{4}$$

where

$$\mu_{ij} = \frac{h\boldsymbol{v}_{ij}\cdot\boldsymbol{r}_{ij}}{c_{s,ij}(r_{ij}^2 + \eta^2)}, \tag{5}$$

and where we use the notation $B - V_{ij} = B - V_i - B - V_j$, $\boldsymbol{r}_{ij} = \boldsymbol{r}_i - \boldsymbol{r}_j$, and $c_{s,ij}$ is the average of the sound speeds for particles i and j. For the simulations we present here, we adopt the parameters $\alpha = \beta = 0.5$ and $\eta = 0.1\ h$. As is typical in artificial viscosity prescriptions, only approaching particles feel a viscous force.

As discussed in SW98, we generally integrate the internal energies using an action-reaction principle,

$$\frac{du_i}{dt} = -\boldsymbol{a}_{i,\,\rm SPH}\cdot\boldsymbol{v}_i, \tag{6}$$

which is formally equivalent to a standard SPH internal energy equation. However, because this approach results in unphysical negative internal energies in a very small number of cases, in that event we use the more standard form

$$\frac{du_i}{dt} = \frac{P_i}{\rho_i^2}\sum_j m_j(1 + \Pi_{ij})\boldsymbol{v}_{ij}\cdot\nabla_i W_{ij} \tag{7}$$

to integrate the internal energy changes. By assuming the sum of the changes in the internal energies of all the particles over a time step (δt_0^n) is directly proportional to the bolometric luminosity of the disk over that same time interval, we can calculate an approximate "light curve" for the simulation

$$L^n = \sum_j \left(\frac{du}{dt}\right)_j^n \delta t_0, \tag{8}$$

where n indicates the time step. Viscous dissipation is a major source of increase for the particles' internal energies, but positive and negative $P\,dV$ work is also included. We note that while our crude approach does yield "light curves" that can be compared with observed light curves, our simulations are only hydrodynamical and contain no radiative transfer, magnetic fields, or truly physical treatment of viscosity. We as a community are still some years away from a fully physical simulation of accretion disk phenomena.

2.2. *The Model Parameters*

FITDisk models the hydrodynamic flow from the inner Lagrange point (L1) onto the primary star M_1 through an accretion

disk. We treat the gravitational potential as the sum of two point masses orbiting around a common center of mass, located at the origin of the coordinate system. In system units, the semimajor axis a is set to 1.0. The calculations are made in the inertial frame, obviating the need to apply Coriolis forces. We typically start the simulations by injecting particles at random locations within a small box that has its back face centered on L1. The injection velocity is the sound speed, scaled to system units. We wish to model a disk at quasi-equilibrium, and so evolve the simulation beginning with an initial burst of particles which may last for several orbits until the desired equilibrium number of particles is in the disk. Anytime a particle is accreted onto M_1 or M_2, or is ejected from the system, it is replaced with a new particle at L1. In this way the system evolves to a dynamical equilibrium.

For the simulations reported here, we injected 1000 particles per orbit until 80,000 particles were in the disk, and from this point on we hold the number of particles at 80,000 by replacing particles that are accreted. We assume a white dwarf mass of 0.80 $M_\odot$ and secondary mass of 0.32 $M_\odot$, placing the mass ratio $q = 0.4$ outside the range that will undergo positive superhumps. The scaled orbital separation is about 1.15 $R_\odot$, and the orbital period is $\sim$3.2 hr, using the approximate secondary mass-radius relation of (Warner 1995), $R_2 \sim M_2^{13/15}$. The disk dynamics, such as relative size, precession rate, etc., are only a function of mass ratio, not the specific masses of the two stars, so these results will be valid for any $q = 0.4$ system. The scaled radius of a 6.9×10^8 cm white dwarf is $R_1 = 0.0086a$.

3. RESULTS

We computed our 80,000 particle simulation out to orbit 200 to allow it to come to equilibrium. We then rotated the particle positions and velocity vectors by 5° about the line of centers between the two stars and restarted the calculation with this tilted disk. We computed two separate runs from this point. The first ("no burst") simulation continued on with a constant $N =$ 80,000 particles, but in order to bring out the negative superhump signal in both the simulation light curve and rendered animation still frames, we computed a second run wherein we introduced a new burst of particles at a rate of 2000 particles per orbit for 10 orbits, bringing the final total of particles to $N =$ 100,000. We continued the simulations out to orbit 250. The top panel of Figure 1 shows the full "light curve" (formally the energy generation as a function of time) of the simulations. The bottom panel of the figure shows the region of interest starting at orbit 200 for both the burst and no-burst cases. It is clear that there is a periodic signal in both light curves, and that the frequency is roughly 2 cycles per orbit, as discussed in Wood et al. (2000).

In Wood et al. (2000) we speculated that the source of the signal was tidal interaction of the rotating tidal field of the secondary star with the tilted disk, but our current simulations prove that idea is not correct. We have since modified our code to write the internal energy change for all particles individually, and color-coding the disk images by this variable clearly shows that the source of the negative superhump signal is the accretion stream disk impact point (the bright spot) as it transits across the face of the tilted disk.

The frequency of the periodic signal in the simulations is roughly twice per orbit, because the light curves in Figure 1 are the sum of the energy generation of all the particles in the simulation and so effectively integrate over 4π sr. For a real observed system, we see only one face of the disk and the accretion stream impact spot as it moves across the visible face of the disk. For an optically thick disk, we do not in general see a signal as the accretion spot moves across the back face of the disk, although this signal may in principle be detectable by sufficiently clever observational techniques. In Burke et al. (1998) we discussed a simple ray-trace method for computing inclination-dependent simulation light curves, in which we rotate all the disk particles about the primary, sort the particles by height within a grid of tubes, and then sum the energy generation of the top few particles in each tube as an approximation to the disk photosphere. In Figure 2 we show several frames from an animation we created (linked in the online version). In this sequence, it is clear that the simulation particles which have the largest energy generation (i.e., are "brightest") are those that in the accretion spot and downstream of the spot, seen here as the particles which have the highest contrast with the image background. Note in particular that these particles form a J-shaped region downstream of the impact spot, and time-series spectroscopy of these systems should be able to probe the dynamics and cooling timescale of this shock-heated gas.

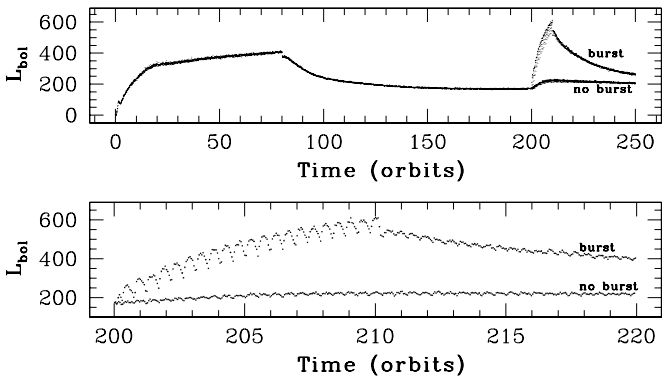

FIG. 1.—Entire simulation "light curve" shown in the top panel. At orbit 200 the simulation was stopped, the disk tilted, and the simulation restarted. In the "no burst" case the simulation continued with 80,0000 particles, whereas in the "burst" case an additional burst of particles was injected, as discussed in the text. The light curves of orbits 200 to 220 for the two cases are shown in the bottom panel. Note that the oscillation is present in both curves, but more dramatic in the "burst" simulation. The simulation negative superhumps have a frequency twice that of the observed superhumps because we effectively integrate over 4π sr. The mass burst of 20,000 additional particles lasts 10 orbits, beyond which particles are again only injected when a particle is accreted. The superhumps are still present but at a lower amplitude.

We use the ray-trace code to produce inclination-dependent light curves of the tilted disk simulation and show the result in Figure 3. In this figure, we show the simulation light curves in the form Δmag versus time for a range of inclinations, as labeled. There are several features to note in this figure. First, the frequency of the periodicity is roughly once per orbit, because for each curve we only "see" one face of the disk. Second, notice that in the top two simulation light curves, which show the results for inclination angles 0° and 180° (i.e., opposite faces of the same disk), the two curves are out of phase with each other, as expected. Finally, while the simulation light curves for inclinations 0° to 60° are very similar, the higher inclination curves 70° and 80° begin to show the effect of the precessing tilted disk interacting with the high-inclination line of sight. These light curves are similar to the observed light curves of negative superhumps (see, e.g., Fig. 6 of Patterson et al. 1997) and perhaps can be used to constrain system parameters on individual systems.

Finally, for a given mass ratio and accretion rate through L1, tilted disks may be physically larger than untilted disks. If the disk is untilted, as it is before orbit 200 in the simulations, the accretion stream deposits low specific angular momentum mass at the outer edge of the disk, which along with tidal torques acts

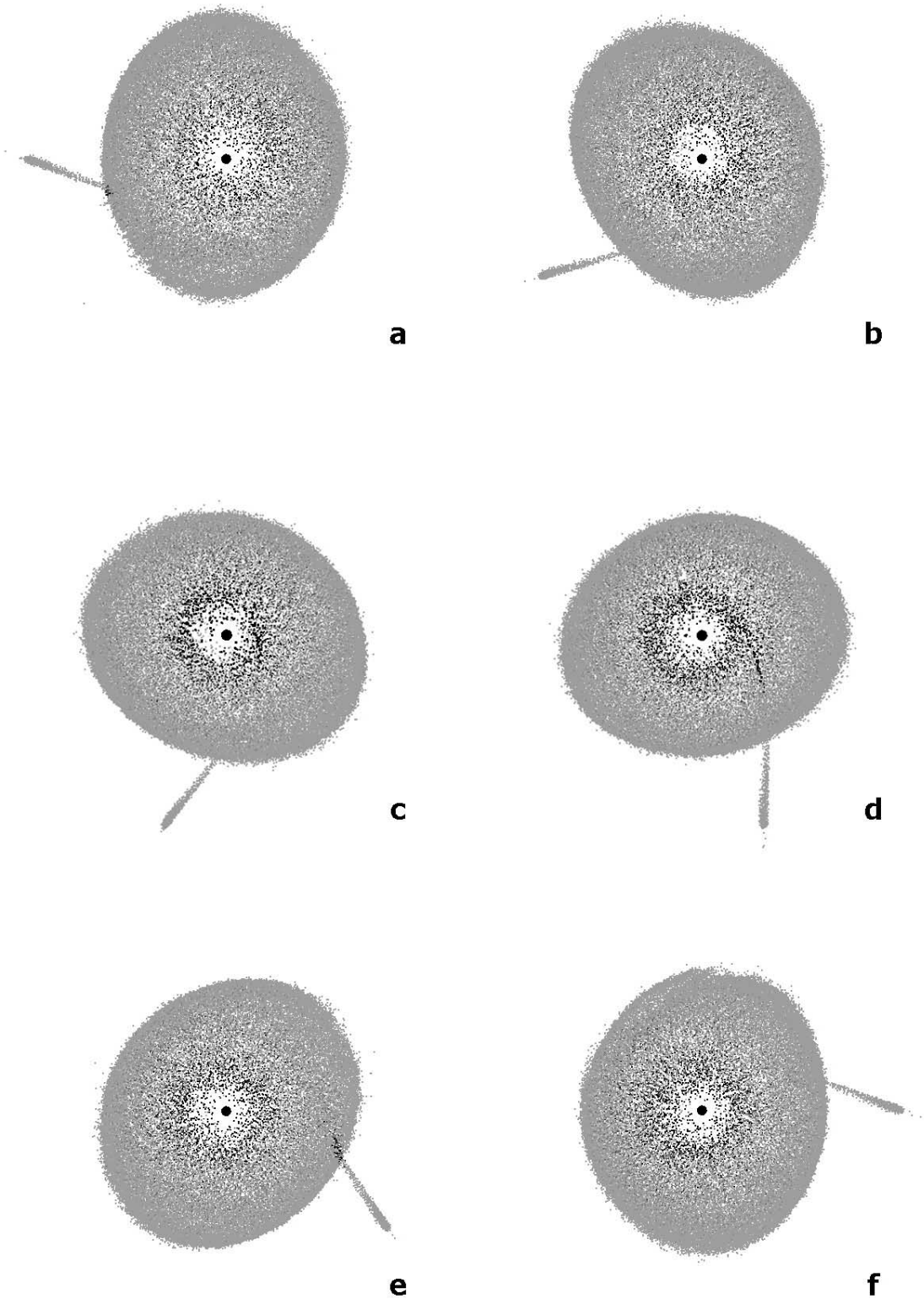

FIG. 2.—One-half orbit of the accretion spot moving across the face of the tilted disk in the inertial frame. In the figure, the viewing angle (inclination) is perpendicular to the orbital plane, and the disk is tilted 5°, such that the line of nodes runs approximately horizontally and is nearly fixed in space over such a short time interval. Toward the top of each panel, the disk is tilted such that the top half is tilted above the plane of the page, above the orbital plane, and toward the bottom of the panel the disk is below the orbital plane. The particles that have the largest energy generation ("brightest") have the largest contrast with the background color. [*This figure is available as an mpeg animation showing 2.5 orbits of this simulation in the electronic edition of the Journal*.]

to constrain the disk radius. Once the disk is tilted, however, most of the angular momentum of the mass in the accretion stream is deposited at smaller radii, as the bright spot sweeps across the face of the disk. Hence, it is possible that a tilted disk could be larger than an equivalent untilted disk, all other parameters being equal. To test this idea, we used some analysis code developed for our recent study of DQ Herculis (Wood et al. 2006). We bin the particle locations for a given time step into 72 sectors of 5° width, and then sort the particles by radius within each sector. In Figure 4 we show the results comparing

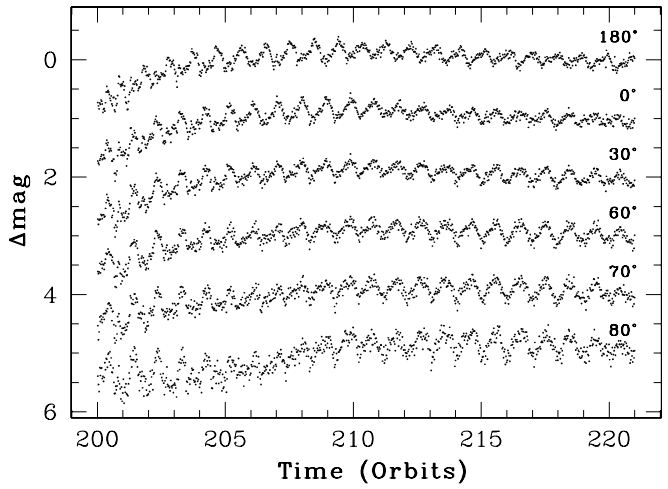

FIG. 3.— Simulation light curves as a function of inclination. The curves have been converted to Δ mag vs. time and offset for clarity. The top two curves demonstrate that the inclination-dependent light curves for opposite faces of the disk are out of phase with each other, as expected (see text). The periodicity is roughly once per orbit in all cases.

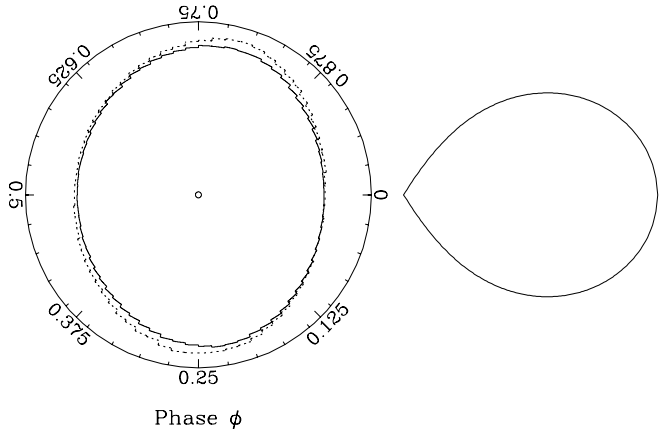

FIG. 4.— Schematic top view of the 95% radius in 72 5° sectors for the untilted equilibrium disk at orbit 200 (*solid line*) and a tilted disk at orbit 240 (*dotted line*). The disk expands slightly in response to the accretion stream depositing low specific angular momentum mass in the inner disk and not only on the disk rim. Also shown are the stellar surfaces (to scale) and a scale showing orbital phase.

the 95% radii for disks at orbit 200 (*solid line*) and at orbit 240 (*dotted line*) for the sequence that did not include a mass burst (i.e., $N = 80{,}000$). For reference we also show the stellar surfaces to scale and a polar axis showing orbital phase.

Clearly, the results show that there is some disk expansion that occurs. Whether or not this would be observationally detectable via eclipse observations is very difficult to predict. Our simulations are purely hydrodynamical, and while our radial sector plots indicate a radial expansion of the disk in certain sectors, we do not calculate a photosphere. Our results suggest that the expansion by eclipse observations should be most easily detected during eclipse egress near phase 0.125.

4. CONCLUSIONS AND DISCUSSION

Our simulations show that, as first suggested by Barrett et al. (1988), the source of the negative superhump signal is the transit of the accretion steam impact spot across the face of the tilted disk. Using a simple ray-trace modification to our SPH code, we find that the negative superhump signals from opposite sides of the disk are out of phase with each other. Because most of the mass flux in the accretion stream is deposited in the inner disk region, the overall disk tilt can persist for a long time, and the disk can expand slightly compared to an untilted disk that has all the low specific angular momentum gas added to the outer disk rim. Time resolved spectroscopy of sufficient resolution should be able to probe the dynamics of the accretion stream impact region, thus improving our understanding of the inner disk region and cooling dynamics of the shock-heated gas.

The cause of the disk tilt in CVs remains unknown, although some form of magnetic field interaction is generally invoked as the most likely explanation. In X-ray binaries, it is reasonably well established that radiation pressure is sufficient to tilt the disk out of the orbital plane, as shown by Maloney et al. (1996) but radiation pressure is too feeble in CVs with white dwarf primaries. In their study of TV Col, Barrett et al. (1988) suggested that the disk tilt might be caused by a magnetic field on the secondary star steering the flow through the L1 region out of the orbital plane. We have found via simulations that this does not lead to a tilted disk, since any geometry that is fixed in the corotating gives an orbit-averaged angular momentum vector perpendicular to the orbital plane. Murray et al. (2002) showed via simulations that instantaneously turning on a magnetic field on the secondary star provide an impulse to the accretion disk perpendicular to the orbital plane that results in a disk tilt. However, again the disk tilt dies away in their simulations because of the inherent symmetry when averaged over several orbits.

We are currently working to understand if *magnetic reconnection events near the L1 region of the secondary star or over the surface of disk itself may provide a sufficient impulse to tilt the accretion disk out of the orbital plane*, and this is planned to be the focus of a future publication. For example, Figure 2 of Hellier & Buckley (1993) shows an "outburst" in TV Col, and the authors determine that the phase of the negative superhumps changed during this event (Hudec et al. [2005] report on the historical outburst record for TV Col). Their conclusion is that this outburst is the result of a factor of $\sim$30 increase in the mass-transfer rate through the L1 region, and this may be part or all of the story, but the light curve shown bears a striking resemblance to a typical flare light curve (Tovmassian et al. 2003), and so this may also be part of the story. Furthermore, the energetics of large flares as compared with the typical kinetic energy of accretion disks suggests this is a viable mechanism, in that large flare events in RS CVn binaries can have energies up to $\sim 10^{37}$ erg (Kozhevnikova et al. 2006; Rubenstein & Schaefer 2000; Mathioudakis et al. 1992), which is within an order of magnitude to an estimated $\sim 10^{38}$ erg for the kinetic energy of an accretion disk (taking the mass of the disk to be $\sim 10^{-10}\,M_{\odot}$ with a typical velocity of 500 km s^{-1}). The flares would in most cases be asymmetic with respect to the orbital plane, and hence capable of providing an impulse perpendicular to the plane, and flare durations are generally short with respect to the orbital periods in the outer disk region.

We thank Vanessa Wilkat, Brian Warner, Suzanne Hawley, Nicole Silvestri, and Michele Montgomery for useful suggestions. We also kindly thank the referee John Thorstenson for his comments and suggestions. This work was supported in part by the National Science Foundation through grant AST–0205902.

REFERENCES

Baker-Branstetter, S., & Wood, M. A. 1999, IAPPP, 76, 31
Barrett, P., O'Donoghue, D., & Warner, B. 1988, MNRAS, 233, 759
Benz, W. 1991, in Lecture Notes in Physics 373, Late Stages of Stellar Evolution: Computational Methods in Astrophysical Hydrodynamics, ed. C. B. de Loore (Berlin: Springer), 259
Bonnet-Bidaud, J. M., Motch, C., & Mouchet, M. 1985, A&A, 143, 313
Burke, C. J., Wood, M. A., & Simpson, J. C. 1998, IAPPP, 71, 44
Hellier, C. 2001, Cataclysmic Variable Stars: How and Why They Vary (Berling: Springer)
Hellier, C., & Buckley, D. A. H. 1993, MNRAS, 265, 766
Hirose, M., & Osaki, Y. 1990, PASJ, 42, 135
Hudec, R., Šimon, V., & Skalický, J. 2005, in ASP Conf. Ser. 330. The Astrophysics of Cataclysmic Variables and Related Objects, ed. J.-M. Hameury & J.-P. Lasota (San Francisco: ASP), 405
Kozhevnikova, A. V., Alekseev, I. Y., Heckert, P. A., & Kozhevnikov, V. P. 2006, Inf. Bull. Variable Stars, 5723, 1
Lattanzio, J. C., Monaghan, J. J., Pongracic, H., & Schwarz, M. P. 1986, J. Sci. Stat. Comput., 7, 591
Lubow, S. H. 1991a, ApJ, 381, 259
———. 1991b, ApJ, 381, 268
Lucy, L. B. 1977, AJ, 82, 1013
Maloney, P. R., Begelman, M. C., & Pringle, J. E. 1996, ApJ, 472, 582
Mathioudakis, M., Doyle, J. G., Avgoloupis, V., Mavridis, L. N., & Seiradakis, J. H. 1992, MNRAS, 255, 48
Monaghan, J. J. 1992, ARA&A, 30, 543
Monaghan, J. J., & Lattanzio, J. C. 1985, A&A, 149, 135
Montgomery, M. M. 2001, MNRAS, 325, 761
———. 2004, Ph.D. thesis, Florida Inst. Tech.
Murray, J. R., Chakrabarty, D., Wynn, G. A., & Kramer, L. 2002, MNRAS, 335, 247
Patterson, J. 1999, in Disk Instabilities in Close Binary Systems, ed. S. Mineshige & J. C. Wheeler (Kyoto: Universal Academy Press), 61
———. 2001, PASP, 113, 736
Patterson, J., Kemp, J., Saad, J., Skillman, D. R., Harvey, D., Fried, R., Thorstensen, J. R., & Ashley, R. 1997, PASP, 109, 468
Patterson, J., Thomas, G., Skillman, D. R., & Diaz, M. 1993, ApJS, 86, 235
Patterson, J., et al. 2002, PASP, 114, 721
———. 2005, PASP, 117, 120
Rubenstein, E. P., & Schaefer, B. E. 2000, ApJ, 529, 1031
Simpson, J. C. 1995, ApJ, 448, 822
Simpson, J. C., & Wood, M. A. 1998, ApJ, 506, 360
Tovmassian, H. M., Zalinian, V. P., Silant'ev, N. A., Cardona, O., & Chavez, M. 2003, A&A, 399, 647
Warner, B. 1995, Cataclysmic Variable Stars (New York: Cambridge Univ. Press)
Whitehurst, R. 1988, MNRAS, 232, 35
———. 1994, MNRAS, 266, 35
Whitehurst, R., & King, A. 1991, MNRAS, 249, 25
Wood, M. A., Dolence, J., & Simpson, J. C. 2006, PASP, 118, 442
Wood, M. A., Montgomery, M. M., & Simpson, J. C. 2000, ApJ, 535, L39